NON-WSSUS VEHICULAR CHANNEL CHARACTERIZATION IN HIGHWAY AND URBAN SCENARIOS AT 5.2 GHZ USING THE LOCAL SCATTERING FUNCTION

Alexander Paier[1], *Thomas Zemen*[3], *Laura Bernadó*[3], *Gerald Matz*[1], *Johan Karedal*[2], *Nicolai Czink*[1,3], *Charlotte Dumard*[3], *Fredrik Tufvesson*[2], *Andreas F. Molisch*[2,4], *Christoph F. Mecklenbräuker*[1]

[1]Institut für Nachrichtentechnik und Hochfrequenztechnik, Technische Universität Wien, Vienna, Austria
[2]Department of Electrical and Information Technology, Lund University, Lund, Sweden
[3]Forschungszentrum Telekommunikation Wien (ftw.), Vienna, Austria
[4]Mitsubishi Electric Research Labs, Cambridge, USA
Contact: apaier@nt.tuwien.ac.at

ABSTRACT

The fading process in high speed vehicular traffic telematic applications at 5 GHz is expected to fulfill the wide-sense stationarity uncorrelated scattering (WSSUS) assumption for very short time-intervals only. In order to test this assumption we apply the concept of a *local* time– and frequency–variant scattering function, which we estimate from measurements of vehicle-to-vehicle wave propagation channels by means of a multi-window spectrogram. The obtained temporal sequence of local scattering functions (LSF) is used to calculate a collinearity measure. We define the *stationarity time* as the support of the region where the collinearity exceeds a certain threshold. The stationarity time is the maximum time duration over which the WSSUS assumption is valid. Measurements from an highway with vehicles driving in opposite directions show stationarity times as small as 23 ms whereas vehicles driving in the same direction show stationarity times of 1479 ms.

1. INTRODUCTION

Reliable delivery of traffic telematic services via IEEE 802.11p is required in a large range of different road traffic scenarios. The wide-sense stationary uncorrelated scattering (WSSUS) assumption [1, 2] is very popular for the simplified description of random linear time-varying channels. Since practical channels never exactly satisfy the WSSUS assumption we consider a *local scattering function* (LSF) which is defined for non-WSSUS channels in [3, 4]. The LSF extends the scattering function [5] of WSSUS channels. Especially for high speed vehicular radio channels the WSSUS assumption is not valid. Due to the high vehicle velocities the wave propagation conditions change rapidly, leading to non stationary channel properties.

Contributions of the paper

- We present estimates of the temporal LSF sequence of a vehicular channel using the concepts from [3, 4]. The vehicular channels were measured in highway and urban environments in Lund, Sweden, during a recent MIMO measurement campaign [6, 7].
- We evaluate the collinearity of this LSF sequence which allows to quantify the time-interval over which the vehicular channel can be approximated as WSSUS. Our method generalizes the approach proposed in [8].

2. MEASUREMENTS

Measurement Equipment

The measurements were carried out with the RUSK LUND channel sounder at a center frequency of 5.2 GHz and with a measurement bandwidth of 240 MHz. As measurement vehicles we used two similar VW LT35 transporters. In Fig. 1 a photograph of the receiver (Rx) vehicle during the measurements is shown. The most important measurement parameters are listed in Tab. 1. A detailed description of the measurement equipment is presented in [6].

Measurement Scenario

For the estimation of the LSF and its correlation function in this paper we consider measurements in three scenarios in Lund, Sweden, and in the surrounding area of Lund. In Scenario 1 the two measurement vehicles were traveling on the highway in opposite directions with a speed of 25 m/s (90 km/h). Fig. 1 presents a photograph of the highway, where we see the receiver vehicle traveling on the lane in opposite direction. Scenario 2 also considers measurement vehicles traveling on the highway with a speed of 25 m/s, but with both vehicles driving in the same direction. In Scenario 3 the two vehicles were traveling in the same direction in an urban environment with a speed of 8.3 m/s (30 km/h). Fig. 2

978-1-4244-1757-5/08/$25.00

Table 1. Measurement configuration parameters.

Center frequency, f_c	5.2 GHz
Measurement bandwidth, BW	240 MHz
Delay resolution, $\Delta\tau = 1/BW$	4.17 ns
Transmit power, P_{Tx}	27 dBm
Test signal length, τ_{max}	3.2 μs
Number of Tx antenna elements, N_{Tx}	4
Number of Rx antenna elements, N_{Rx}	4
Snapshot time, t_{snap}	102.4 μs
Snapshot repetition rate, t_{rep}	307.2 μs
Number of snapshots in time, S'	32500
Number of sample in frequency domain, N'	769
Recording time, t_{rec}	10 s
File size, FS	1 GB
Tx antenna height, h_{Tx}	2.4 m
Rx antenna height, h_{Rx}	2.4 m

Fig. 1. Photograph of the highway from Scenario 1 and 2.

depicts a photograph of Scenario 3. A further description of the measurement scenarios as well as satellite photographs can be found in [6]. A summary of the measurement scenario properties is shown in Tab. 2.

Table 2. Measurement scenario properties.

Scenario	Environment	Driving direction	Velocity
1	Highway	Opposite direction	25 m/s (90 km/h)
2	Highway	Same direction	25 m/s (90 km/h)
3	Urban	Same direction	8.3 m/s (30 km/h)

Measurement Evaluation

The sampled channel transfer function of a linear time-variant channel $\mathbf{H}$

$$L_{\mathbf{H}}[m, q] = L_{\mathbf{H}}(mt_{\text{rep}}, q/(N\Delta\tau)) \tag{1}$$

is measured by the channel sounder and stored over a duration of $t_{\text{rec}} = 10\,\text{s}$, with time index $m \in \{0 \dots S' - 1\}$ and frequency index $q \in \{-(N'-1)/2 \dots (N'-1)/2\}$. We obtain the complex sampled channel impulse response

$$h[m, n] = h(mt_{\text{rep}}, n\Delta\tau) \tag{2}$$

Fig. 2. Photograph of the Scenario 3.

by means of an inverse Fourier transform using a Hanning windowing function. No significant signal components were measured for delays larger than 1 μs, hence we consider only the first $N = 256$ delay samples, $n \in \{0, \dots, N-1\}$. The time index m was limited to a segment with time duration of $t_{\text{seg}} = 2\,\text{s}$ for all three scenarios, $m \in \{0, \dots, S-1\}$ with $S = 6500 = S' t_{\text{seg}}/t_{\text{rec}}$.

We performed measurements with 4 antenna elements at the transmitter (Tx) side and 4 antenna elements at the receiver side. For the estimation of the LSF and its correlation function in this paper we consider only a single antenna link out of this set of 16 individual channels. In the case of Scenario 1 we investigate the channel between the antenna elements whose main lobes are facing towards each other, when the vehicles are approaching. In the other two Scenarios 2 and 3 we consider also a channel where the elements are facing towards each other during the whole time duration of 2 s, see [6, Fig. 1].

Fig. 3 (a) - (c) present the power-delay profiles (PDPs) over time for each of the three scenarios. The PDP at a specific time instant is based on the impulse repsonses over a time duration of 20 ms. In Fig. 3 (a) we observe a strong line of sight (LOS) path with decreasing delay until approximately 0.5 s and increasing delay afterwards, and some paths with larger delays resulting from scattering, e.g. a group of scattered paths at a delay of approximately 600 ns. From the characteristic of the LOS path in this figure we observe the passing time of the two vehicles at approximately 0.5 s. In Scenario 2 and 3, Fig. 3 (b) and (c), the vehicles were driving in the same direction, therefore the delay of the LOS path is staying approximately constant over the considered time of 2 s. In Scenario 2, the highway environment, we measured only one path beside the LOS path, also with constant delay over time, occurring approximately 50 ns after the LOS path. In Fig. 3 (c), the urban environment, we observe some discrete paths with time varying delays and also contributions from diffuse scattering. This means that in the urban environment there are much more significant scatterers[1] than in the

[1]When speaking of "scatterers", we mean any objects that redirect elec-

considered highway environment.

3. LOCAL SCATTERING FUNCTION

The WSSUS assumption is a very popular assumption allowing for a simplified description of random linear time-varying channels. Especially for high speed vehicular radio channels the WSSUS assumption is not valid. In this paper we use the concept of a LSF which is defined for non-WSSUS channels in [3] for continuous time as

$$\mathcal{C}_{\mathbf{H}}(t,f;\tau,\nu) = \int_{-\infty}^{\infty}\int_{-\infty}^{\infty} R_h(t,\tau;\Delta t,\Delta\tau) \times \mathrm{e}^{-\mathrm{j}2\pi(\nu\Delta t+f\Delta\tau)}\mathrm{d}\Delta t\,\mathrm{d}\Delta\tau\,, \quad (3)$$

where

$$R_h(t,\tau;\Delta t,\Delta\tau) = \mathsf{E}\{h(t,\tau+\Delta\tau)h^*(t-\Delta t,\tau)\} \quad (4)$$

is the 4-D covariance function and $\mathsf{E}\{\cdot\}$ denotes mathematical expectation, i.e., ensemble averaging.

Local Scattering Function Estimator

As explained in [3] the LSF is not guaranteed to be positive and furthermore depends on the whole correlation function $R_h(t,\tau;\Delta t,\Delta\tau)$. Therefore, [3] additionally defines a generalized LSF based on K linear time-variant prototype systems $\boldsymbol{G}_k$ whose transfer function $L_{\boldsymbol{G}_k}(t,f)$ is smooth and localized about the origin of the time-frequency plane. This means $\boldsymbol{G}_k$ amounts to a temporally localized low-pass filter.

The generalized LSF is defined as

$$\mathcal{C}_{\mathbf{H}}^{(\Phi)}(t,f;\tau,\nu) = \mathsf{E}\left\{\sum_{k=0}^{K-1}\gamma_k\left|\mathcal{H}^{(\boldsymbol{G}_k)}(t,f;\tau,\nu)\right|^2\right\}, \quad (5)$$

where

$$\mathcal{H}^{(\boldsymbol{G}_k)}(t,f;\tau,\nu) = \mathrm{e}^{\mathrm{j}2\pi f\tau}\int_{-\infty}^{\infty}\int_{-\infty}^{\infty} L_{\mathbf{H}}(t',f') \times L^*_{\boldsymbol{G}_k}(t'-t,f'-f)\mathrm{e}^{-\mathrm{j}2\pi(\nu t'-\tau f')}\mathrm{d}t'\mathrm{d}f' \quad (6)$$

and the coefficients γ_k need to fulfill the condition

$$\sum_{k=0}^{K-1}\gamma_k = 1\,. \quad (7)$$

From (6) it becomes clear that the generalized LSF can be interpreted as an expected multi-window spectrogram [9, 10] of $\mathbf{H}$. This interpretation allows to obtain a practical estimation method [4] which we will use for our vehicular channel

tromagnetic radiation into a different direction, including specular reflectors and diffracting edges. A more precise formulation would be "interacting objects".

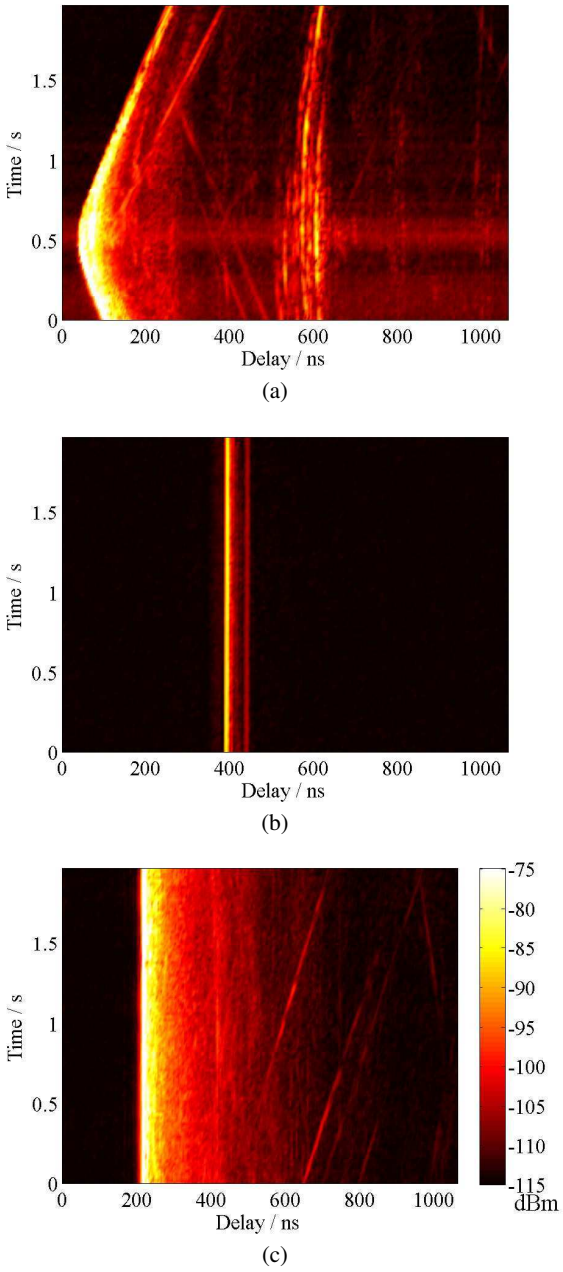

Fig. 3. Average PDPs of (a) Scenario 1, (b) Scenario 2, and (c) Scenario 3.

measurements. From now on we will omit the explicit dependence of $\mathcal{C}_{\mathbf{H}}$ on f considering the dependence of the LSF on t only.

We use a discrete time implementation of the scattering function estimator described in [4]. The temporally localized low-pass filters $\boldsymbol{G}_k$ are represented by the sampled transfer function

$$L_{\boldsymbol{G}_k}[m,q] = L_{\boldsymbol{G}_k}(mt_{\mathrm{rep}}, \frac{q}{N\Delta\tau}) \tag{8}$$

for $q \in \{-N/2 \dots N/2-1\}$. We apply the discrete time equivalent of the separable transfer function used in [4]:

$$L_{\boldsymbol{G}_k}[m,q] = u_i[m+M/2]\tilde{u}_j[q+N/2]\,, \tag{9}$$

where $k = iJ+j$, $i \in \{0 \dots I-1\}$, and $j \in \{0 \dots J-1\}$. The sequences $u_i[m]$ are the discrete prolate spheroidal (DPS) sequences with concentration in the interval $\mathcal{I}_M = \{0 \dots M-1\}$ and bandlimited to $[-I/M, I/M]$, defined as [11]

$$\sum_{\ell=0}^{M-1} \frac{\sin(2\pi I/M(\ell-m))}{\pi(\ell-m)} u_i[\ell] = \lambda_i u_i[m]\,. \tag{10}$$

The sequences $\tilde{u}_j[q]$ are defined similarly with concentration in the interval $\mathcal{I}_N$ and bandlimited to $[-J/N, J/N]$.

The multi-window spectrogram is computed according to

$$\mathcal{C}_{\mathbf{H}}^{(\Phi)}[m;n,p] = \frac{1}{IJMN} \sum_{k=0}^{K-1} \left| \mathcal{H}^{(\boldsymbol{G}_k)}[m;n,p] \right|^2 \tag{11}$$

with $n \in \{0,\dots,N-1\}$ and $p \in \{-M/2,\dots M/2-1\}$ where

$$\mathcal{H}^{(\boldsymbol{G}_k)}[m;n,p] = \sum_{m'=-M/2}^{M/2-1} \sum_{q'=-N/2}^{N/2-1} L_{\mathbf{H}}[m',q'] \times L_{\boldsymbol{G}_k}[m'-m,q'] \mathrm{e}^{-\mathrm{j}2\pi(pm'-nq')}\,. \tag{12}$$

Note that $L_{\mathbf{H}}[m,q] = L_{\mathbf{H}}(mt_{\mathrm{rep}}, \frac{q}{N\Delta\tau})$ and $\mathcal{C}_{\mathbf{H}}^{(\Phi)}[m;n,p] = \mathcal{C}_{\mathbf{H}}^{(\Phi)}(mt_{\mathrm{rep}}; n\Delta\tau, \frac{p}{Mt_{\mathrm{rep}}})$.

4. MEASUREMENT RESULTS FOR THE LOCAL SCATTERING FUNCTION

We estimate the LSF from noisy measurements using (11). As temporal windows we use $I = 5$ DPS sequences with energy concentration in an interval with length $M = 64$ assuming a lower bound of the *stationarity time* of $T_S > Mt_{\mathrm{rep}} = 19.2\,\mathrm{ms}$. In the frequency domain we used $J = 1$ DPS sequence with concentration in the interval with length $N = 256$ assuming a *stationarity bandwidth* of $F_S > 240\,\mathrm{MHz}$. This assumption can be justified by the fact that 240 MHz corresponds to less than 5% relative bandwidth and the antenna voltage standing wave ratio (VSWR) varies by less than 1 dB over the measurement bandwidth. With these assumptions

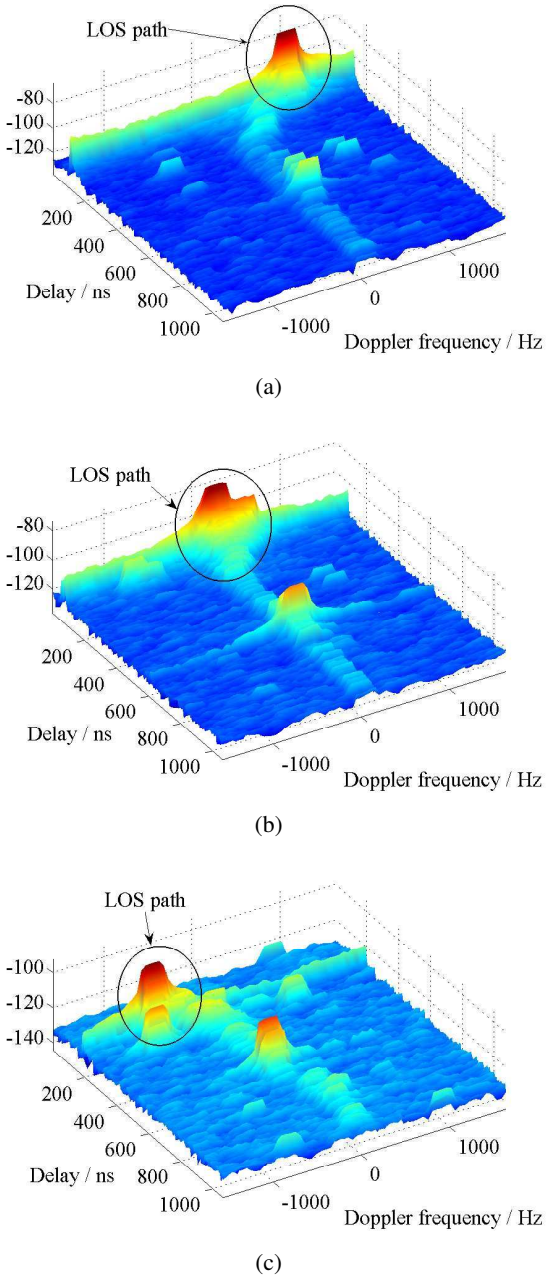

Fig. 4. Estimated generalized LSF for different time snapshots in Scenario 1: (a) $t = 0\,\mathrm{s}$, (b) $t = 0.5\,\mathrm{s}$, and (c) $t = 1.5\,\mathrm{s}$

we achieve a Doppler resolution of 51 Hz for the generalized LSF.

The estimated generalized LSF can directly be related to the propagation scenario. In the following we describe the estimated generalized LSF by means of the measurement in Scenario 1. Figure 4 presents the estimated generalized LSF from Scenario 1 for three different time snapshots: (a) $t = 0$ s — vehicles are approaching, (b) $t = 0.5$ s — vehicles are passing and (c) $t = 1.5$ s — vehicles are leaving.

We can explain the time variance of the generalized LSF by focusing on the LOS path. In Figure 4 (a) the LOS path has a delay of approximately 110 ns and a Doppler of frequency of approximately 865 Hz. This Doppler frequency agrees exactly with our intended speed of 50 m/s, 25 m/s for each of the two vehicles. Figure 4 (b) shows a LOS path with reduced delay (approximately 60 ns) — vehicles are now closer together — and a Doppler of frequency near to 0 Hz. In this passing scenario the LOS path wave propagation is perpendicular to the driving direction. We can observe an increased delay of approximately 190 ns in Figure 4 (c) and a Doppler frequency of approximately -815 Hz. In this case the relative speed between the two vehicles is a little bit lower than the intended speed of 50 m/s. The negative Doppler frequency confirms that the vehicles are leaving at this time.

Beside this strong LOS path in Fig. 4 we can also observe smaller paths with variant delays and Doppler frequencies, which also indicate the time variance of the generalized LSF, and therefore a non-stationary channel.

5. COLLINEARITY OF THE GENERALIZED LOCAL SCATTERING FUNCTION SEQUENCE

The collinearity of the generalized LSF sequence between two time instances allows to quantify the dimension of the stationarity region in time, i.e. the stationarity time T_s of the non-WSSUS fading process. For the duration of the stationarity time simplified WSSUS models can be applied. Note that the stationarity time will be itself time-variant $T_s[m]$ since it depend on the changing wave propagation environment.

In [8] the PDP is used to obtain an estimate of the stationarity time of the fading process. We extend this approach by using the generalized LSF which incorporates dispersion in delay and Doppler.

To obtain estimates for the time-variant stationarity time $T_s[m]$ we proceed in two steps. First we compute collinearity of the generalized LSF sequence. Secondly we set a threshold for the collinearity. Similar to [8] we define the *stationarity time* as the support of the region where the collinearity exceeds a certain threshold. Furthermore we need to validate that the lower bound $T_s > 19.4$ ms is a valid choice.

We stack all MN elements of the generalized LSF $\mathcal{C}_{\mathbf{H}}^{(\Phi)}$ in the vector $\boldsymbol{c}_{\mathbf{H}}[m]$ computing the collinearity of the generalized LSF

$$R_{\mathcal{C}_{\mathbf{H}}}[m_1, m_2] = \frac{\boldsymbol{c}_{\mathbf{H}}[m_1]^{\mathrm{T}} \boldsymbol{c}_{\mathbf{H}}[m_2]}{\|\boldsymbol{c}_{\mathbf{H}}[m_1]\| \|\boldsymbol{c}_{\mathbf{H}}[m_2]\|} \tag{13}$$

for two time instances m_1 and m_2, i.e. a distance measure in Hilbert space.

We calculate $R_{\mathcal{C}_{\mathbf{H}}}[m_1, m_2]$ using a step size of $\Delta m = 10$, $m_1 = \Delta m m_1'$ and $m_2 = \Delta m m_2'$ for $m_1', m_2' \in \{0 \dots S/\Delta m - 1\}$ to limit the computational complexity

6. STATIONARITY TIME ESTIMATES

Fig. 5 (a) - (c) present the collinearity of the generalized LSF between two time instances m_1 and m_2 for each of the three scenarios in logarithmic scale. In Fig. 5 (a) we observe a strong decrease of the collinearity away from the main diagonal. This means that two generalized LSF at different time snapshots show a high correlation only for a very small time difference between the generalized LSFs. Fig. 5 (b) and (c) present a much higher correlation over longer time differences. Special attention should be paid to the different logarithmic scale for the color maps of the three scenarios. In Scenario 1 the collinearity decreases much faster than in the other two scenarios. Remember that in Scenario 1 the vehicles are going in opposite directions and in Scenario 2 and 3 the vehicles are going in the same direction.

As mentioned above the 2D plot of the collinearity of Scenario 2 and 3 both show higher correlation in time. The collinearity matrix of Scenario 2 can be described as more or less homogeneous over the 2 s time duration, whereas the collinearity matrix of Scenario 3 has a time-variant structure. This can be explained by the existence of much more scatterers in Scenario 3 than in Scenario 2, as described in Sec. 2. A comparison of Fig. 5 (b), (c) and Fig. 3 (b), (c) shows this difference in the number of scatterers too.

In order to estimate the *stationarity time* we have to set a threshold for the collinearity. Similar to [8] we define the *stationarity time* as the support of the region where the collinearity exceeds a certain threshold.

We define the indicator function

$$\gamma[m', \tilde{m}] = \begin{cases} 1 & : \quad R_{\mathcal{C}_{\mathbf{H}}}[m', m' + \tilde{m}] > c_{\mathrm{thres}} \\ 0 & : \quad \text{otherwise} \end{cases} \tag{14}$$

to calculate the (time-variant) *stationarity-time* as

$$T_s[m'] = \Delta m t_{\mathrm{rep}} \sum_{\tilde{m}=-S/\Delta m-1}^{S/\Delta m-1} \gamma[m', \tilde{m}] \tag{15}$$

In contrast to the spatial distance expression in [8] we specify a *stationarity time*. Spatial distances are difficult to compare if both, transmitter and receiver, are moving. For the estimation of the stationarity time we assume a threshold of $c_{\mathrm{thres}} = 0.9$ ($10 \log(0.9) = -0.46$).

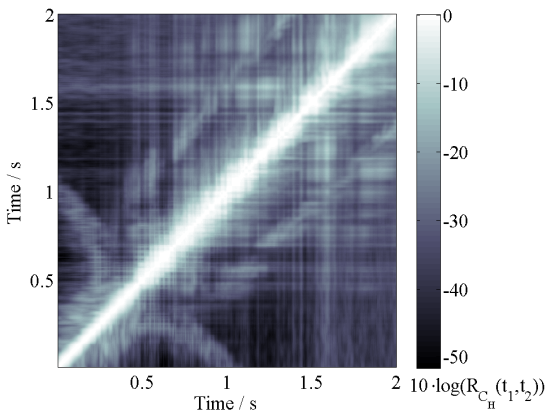

(a)

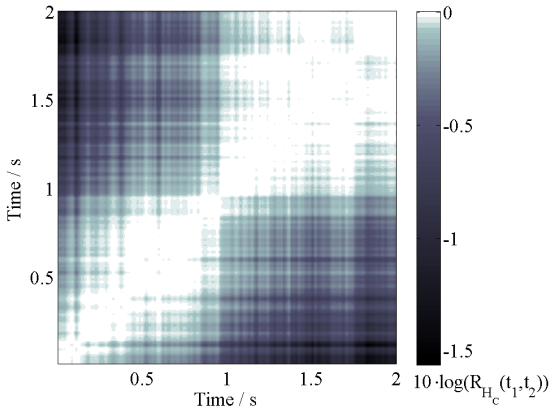

(b)

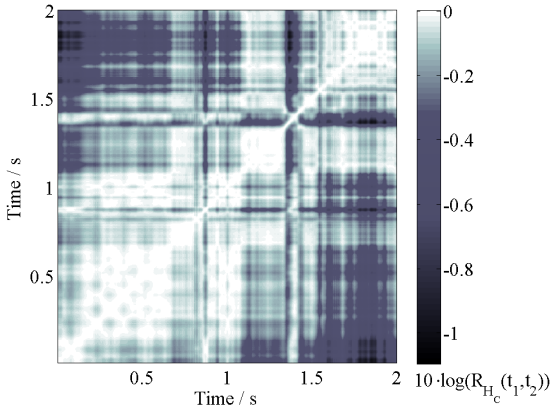

(c)

Fig. 5. Estimated collinearity of the generalized LSF of (a) Scenario 1, (b) Scenario 2, and (c) Scenario 3 (note the different color scales).

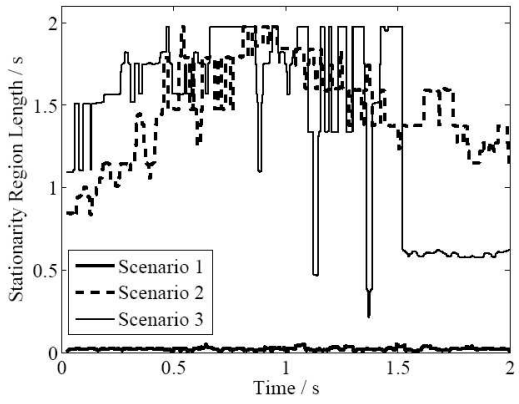

Fig. 6. LRS of all three scenarios

Fig. 6 shows the time-variant stationarity time for each of the three scenarios over the duration of 2 s. We observe a very short stationarity time with a mean of 23 ms for Scenario 1. Scenario 2 shows a mean stationarity time of 1479 ms and Scenario 3 a mean time of 1412 ms.

In the case of Scenario 1, where the vehicles are traveling in opposite directions we achieve a very short stationarity time. Scenario 2 and 3, where both vehicles are traveling in the same direction, show a longer stationarity time. It is interesting that the stationarity times of these two scenarios are in a similar range, because the number of scatterers in these scenarios is very different — only a few scatterers in Scenario 2 and a lot of scatterers in Scenario 3. In this case we also have to consider the different speed of the vehicles in the two scenarios — 25 m/s in Scenario 2 and 8.3 m/s in Scenario 3. This means that the vehicles in Scenario 2 cover a larger distance as in Scenario 3.

7. CONCLUSIONS

We applied the concept of a *local* scattering function (LSF) to characterize real-world vehicular channels from measurements in high-speed scenarios. We observed rapid variations of the line of sight path in the delay-Doppler domain. In order to estimate the stationarity time, we estimated the collinearity of the temporal LSF sequence. We found a very short mean stationarity time of 23 ms for a highway scenario, where the vehicles were traveling in opposite directions. In the same environment, but with both vehicles driving in the same direction, we got a much higher mean stationarity time of 1479 ms. For an urban scenario, also with both vehicles driving in the same direction, but with a speed of one third compared with the speed on the highway, we estimated a mean stationarity time of 1412 ms which is in the same range as on the highway. We conclude that there is a large difference in the time

of stationarity if the vehicles are going in same or in opposite directions. It is also noteworthy that the popular tapped-delay channel models assume the validity of WSSUS, and can therefore only be used within a stationarity time. A more general modeling approach that is not restricted by these concerns will be given in [12].

8. ACKNOWLEDGMENTS

We would like to thank Ernst Bonek for continuous encouragement and support and for pointing us to [8]. We would like to thank RIEGL Laser Measurement Systems GmbH and MEDAV GmbH for their generous support. This work was carried out with partial funding from Kplus and the Vienna Science and Technology Fund (WWTF) in the ftw. projects I-0 and COCOMINT and partially by an INGVAR grant of the Swedish Strategic Research Foundation (SSF), and the SSF Center of Excellence for High–Speed Wireless Communications (HSWC). Finally, we would like to thank Helmut Hofstetter for helping with the measurements and the COST Action 2100.

9. REFERENCES

[1] P. A. Bello, "Characterization of randomly time-variant linear channels," *IEEE Transactions on Communications*, vol. 11, pp. 360–393, 1963.

[2] R. Kattenbach, "Charakterisierung zeitvarianter Indoor-Funkkanäle anhand ihrer System- und Korrelationsfunktionen," Ph.D. dissertation, Universitätsgesamthochschule Kassel, 1997.

[3] G. Matz, "On non-WSSUS wireless fading channels," *IEEE Transactions on Wireless Communications*, vol. 4, pp. 2465–2478, September 2005.

[4] ——, "Doubly underspread non-WSSUS channels: Analysis and estimation of channel statistics," in *Proc. IEEE Int. Workshop Signal Processing Advance Wireless Communications (SPAWC)*, Rome, Italy, June 2003, pp. 190–194.

[5] A. F. Molisch, *Wireless Communications*. IEEE-Press - Wiley and Sons, 2005.

[6] A. Paier, J. Karedal, N. Czink, H. Hofstetter, C. Dumard, T. Zemen, F. Tufvesson, C. F. Mecklenbräuker, and A. F. Molisch, "First results from car-to-car and car-to-infrastructure radio channel measurements at 5.2 GHz," in *International Symposium on Personal, Indoor and Mobile Radio Communications (PIMRC) 2007*, September 2007, pp. 1–5.

[7] A. Paier, J. Karedal, N. Czink, H. Hofstetter, C. Dumard, T. Zemen, F. Tufvesson, A. F. Molisch, and C. F. Mecklenbräuker, "Car-to-car radio channel measurements at 5 GHz: Pathloss, power-delay profile, and delay-Doppler spectrum," in *IEEE International Symposium on Wireless Communication Systems (ISWCS)*, October 2007, pp. 224–228.

[8] A. Gehring, M. Steinbauer, I. Gaspard, and M. Grigat, "Empirical channel stationarity in urban environments," in *Proc. Eur. Personal Mobile Communications Conf. (EPMCC)*, Vienna, Austria, February 2001.

[9] D. J. Thomson, "Spectrum estiamtion and harmonic analysis," vol. 70, no. 9, pp. 1055–1096, September 1982.

[10] D. B. Percival and A. T. Walden, *Spectral Analysis for Physical Applications*. Cambridge University Press, 1963.

[11] D. Slepian, "Prolate spheroidal wave functions, Fourier analysis, and uncertainty - V: The discrete case," *The Bell System Technical Journal*, vol. 57, no. 5, pp. 1371–1430, May-June 1978.

[12] J. Karedal, F. Tufvesson, A. F. Molisch, N. Czink, A. Paier, C. F. Mecklenbräuker, C. Dumard, and T. Zemen, "A geometry-based stochastic MIMO model for vehicle-to-vehicle communications," *IEEE Transactions on Wireless Communications*, 2008, to be submitted.